

Numerical investigation on threading dislocation bending with InAs/GaAs quantum dots

Guo-Feng Wu(武国峰), Jun Wang(王俊), Wei-Rong Chen(陈维荣), Li-Na Zhu(祝丽娜), Yuan-Qing Yang(杨苑青), Jia-Chen Li(李家琛), Chun-Yang Xiao(肖春阳), Yong-Qing Huang(黄永清), Xiao-Min Ren(任晓敏), Hai-Ming Ji(季海铭), and Shuai Luo(罗帅)

Citation: Chin. Phys. B, 2021, 30 (**11**): 110201. DOI: 10.1088/1674-1056/abfd9f
Journal homepage: http://cpb.iphy.ac.cn; http://iopscience.iop.org/cpb

What follows is a list of articles you may be interested in

A meshless model for transient heat conduction analyses of 3D axisymmetric functionally graded solids

Li Qing-Hua, Chen Shen-Shen, Zeng Ji-Hui
Chin. Phys. B, 2013, 22 (**12**): 120204. DOI: 10.1088/1674-1056/22/12/120204

A complex variable meshless local Petrov-Galerkin method for transient heat conduction problems

Wang Qi-Fang, Dai Bao-Dong, Li Zhen-Feng
Chin. Phys. B, 2013, 22 (**8**): 080203. DOI: 10.1088/1674-1056/22/8/080203

An improved local radial point interpolation method for transient heat conduction analysis

Wang Feng, Lin Gao, Zheng Bao-Jing, Hu Zhi-Qiang
Chin. Phys. B, 2013, 22 (**6**): 060206. DOI: 10.1088/1674-1056/22/6/060206

The discontinuous Petrov-Galerkin method for one-dimensional compressible Euler equations in the Lagrangian coordinate

Zhao Guo-Zhong, Yu Xi-Jun, Guo Peng-Yun
Chin. Phys. B, 2013, 22 (**5**): 050206. DOI: 10.1088/1674-1056/22/5/050206

Combine complex variable reproducing kernel particle method and finite element method for solving transient heat conduction problems

Chen Li, Ma He-Ping, Cheng Yu-Min
Chin. Phys. B, 2013, 22 (**5**): 050202. DOI: 10.1088/1674-1056/22/5/050202

Numerical investigation on threading dislocation bending with InAs/GaAs quantum dots*

Guo-Feng Wu(武国峰)[1], Jun Wang(王俊)[1,†], Wei-Rong Chen(陈维荣)[1], Li-Na Zhu(祝丽娜)[1], Yuan-Qing Yang(杨苑青)[1], Jia-Chen Li(李家琛)[1], Chun-Yang Xiao(肖春阳)[1], Yong-Qing Huang(黄永清)[1], Xiao-Min Ren(任晓敏)[1], Hai-Ming Ji(季海铭)[2], and Shuai Luo(罗帅)[2]

[1] *State Key Laboratory of Information Photonics and Optical Communications, Beijing University of Posts and Telecommunications, Beijing* 100876, *China*

[2] *Center of Materials Science and Optoelectronics Engineering, University of Chinese Academy of Sciences, Beijing* 100049, *China*

(Received 27 January 2021; revised manuscript received 23 April 2021; accepted manuscript online 1 May 2021)

The threading dislocations (TDs) in GaAs/Si epitaxial layers due to the lattice mismatch seriously degrade the performance of the lasers grown on silicon. The insertion of InAs quantum dots (QDs) acting as dislocation filters is a pretty good alternative to solving this problem. In this paper, a finite element method (FEM) is proposed to calculate the critical condition for InAs/GaAs QDs bending TDs into interfacial misfit dislocations (MDs). Making a comparison of elastic strain energy between the two isolated systems, a reasonable result is obtained. The effect of the cap layer thickness and the base width of QDs on TD bending are studied, and the results show that the bending area ratio of single QD (the bending area divided by the area of the QD base) is evidently affected by the two factors. Moreover, we present a method to evaluate the bending capability of single-layer QDs and multi-layer QDs. For the QD with 24-nm base width and 5-nm cap layer thickness, taking the QD density of 10^{11} cm^{-2} into account, the bending area ratio of single-layer QDs (the area of bending TD divided by the area of QD layer) is about 38.71%. With inserting five-layer InAs QDs, the TD density decreases by 91.35%. The results offer the guidelines for designing the QD dislocation filters and provide an important step towards realizing the photonic integration circuits on silicon.

Keywords: InAs/GaAs quantum dots, threading dislocation, finite element method, bending area

PACS: 02.70.Dh, 03.65.Db, 61.50.Ah, 81.05.Ea **DOI:** 10.1088/1674-1056/abfd9f

1. Introduction

With the advent of the era of big data and the rapid growth of internet information, communication networks are required to develop towards the high speed and large capacity.[1,2] Owing to the limitation of transmission bandwidth and power consumption, the traditional electrical interconnection cannot meet the development requirements for high-performance chips, and integrated optical interconnection on Si platform is considered as one of the effective ways to solve these problems.[3,4] As the core device of optoelectronic integration, heteroepitaxial laser on GaAs/Si template can integrate the advantages of the two materials to realize the Si-based monolithic integration of microelectronic devices and the GaAs-based optoelectronic devices, and it is widely used in the high bandwidth optical interconnection field.[5,6]

However, the GaAs/Si heteroepitaxy encounters many difficulties, in which the major bottleneck problem required to be solved is the high-density threading dislocations (TDs) due to the substantial difference in lattice constants between the two materials. If there are a large number of dislocations in the epitaxial layer, the minority carriers will form non-radiation recombination before the population inversion, which will seriously affect the performance of laser.[7] Therefore, it is necessary to take measures to reduce the density of TDs. In the past 40 years, various methods have been proposed for TD bending, such as thermal cyclic annealing, patterning substrates, and using strained-layer superlattices (SLS) and QDs.[8–14] Compared with SLS, QDs have strong stress field as three-dimensional stress structures. A very strong Peach–Koehlor force will bend the dislocation energetically when a TD propagates close to a QD.[15–18]

To reduce the TD density, the design of QD dislocation filters has attracted extensive attention. Experimentally, Wang *et al*. measured the dislocation density to be about 2×10^6 cm^{-2} by inserting five-layer InAs QDs dislocation filters into GaAs/Si film while the the dislocation density is 5×10^7 cm^{-2} in the sample without QDs.[19] By the theoretical analysis and further optimizing the experimental condition, Hu *et al*. reduced dislocation density from 3×10^6 cm^{-2} to 9×10^5 cm^{-2} by combining the insertion of three-layer InAs

*Project supported by the National Natural Science Foundation of China (Grant Nos. 61874148, 61974141, and 61674020), the Beijing Natural Science Foundation, China (Grant No. 4192043), the National Key Research and Development Program of China (Grant No. 2018YFB2200104), the Fund from the Beijing Municipal Science & Technology Commission, China (Grant No. Z191100004819012), the Project of the State Key Laboratory of Information Photonics and Optical Communications, Beijing University of Posts and Telecommunications, China (Grant No. IPOC2018ZT01), and the 111 Project of China (Grant No. B07005).

†Corresponding author. E-mail: wangjun12@bupt.edu.cn

© 2021 Chinese Physical Society and IOP Publishing Ltd

QDs dislocation filters with the three-step growth method.[20] Theoretically, Ye *et al*. analyzed the TD bending in GaN/AlN QDs by using the finite element method (FEM), in which the misfit strain introduced by the edge dislocation is modeled by feeding Eshelby strain into this system.[21] Yang *et al*. used the position independent model (PIM) to calculate the bending area ratio of single $In_xGa_{1-x}As$/GaAs QD.[18] Zhou *et al*. investigated the effect of $In_xGa_{1-x}As$/GaAs QDs component on the obstruction of TDs by adopting FEM model.[22]

In short, the dislocation density is reduced with using the embedded QDs dislocation filter, and the TD bending is observed by transmission electron microscopy (TEM). However, the effect of dislocation filters cannot be anticipated before the crystal growth. Evaluating the bending capability can not only help us to improve the performance of QD dislocation filters thereby avoiding the poor effect in experiment, but also shorten the experiment time and reduce cost. Whereas according to the reports, the theoretical study about edge dislocation is unsuitable for the analysis of TD bending in a GaAs/Si epitaxial system. The position of TD is ignored by the PIM method, but its position plays an important role in determining the elastic strain energy.[23] More importantly, these researches are limited to single QD, which cannot provide enough help for the design of dislocation filters in experiment.

From what has been discussed above, in this study, the full consideration is devoted to the influence of dislocation position, and the finite element method (FEM) is used to establish the three-dimensional (3D) model of 60° TD, and the critical condition for TD inclination is studied. What is more, the method to evaluate the bending capability of single-layer QDs and multi-layer QDs is proposed.

In the first part of this paper, the critical position for TD bending is determined by the FEM calculation. Next, the influence of cap layer thickness and QD base width are discussed, and the results indicate that the increase of them makes positive contribution to TD bending. Finally, the bending area ratio of single-layer QDs and the dislocation blocking ratio of multi-layer QDs (TDs impeded by QDs dislocation filter divide by the initial TDs) are predicted.

2. Model and methods

The previous researches show that the boundary effect can be effectively avoided if the volume of the substrate is much larger than QD, and the initial stress in the substrate can also be considered to be zero.[24–26] Therefore, we establish a cubic GaAs substrate with a size of 100 nm×100 nm×100 nm including 0.3-nm wetting layer (usually $1\sim2$ monolayers[24]). A 4-nm-high tapered InAs QD is located in the center above the substrate. The width of the QD ranges from 8 nm–24 nm, and the thickness of cap layer is 5 nm. Note that the effect of cap layer thickness will be studied in the later section, in which the different thickness is also analyzed. In our work, Cartesian coordinates are adopted and the origin is seated the center of the substrate bottom. The X axis, Y axis, and Z axis represent [110], [-110], and [001] directions, respectively, where Z direction is the growth direction of QD as shown in Fig. 1.

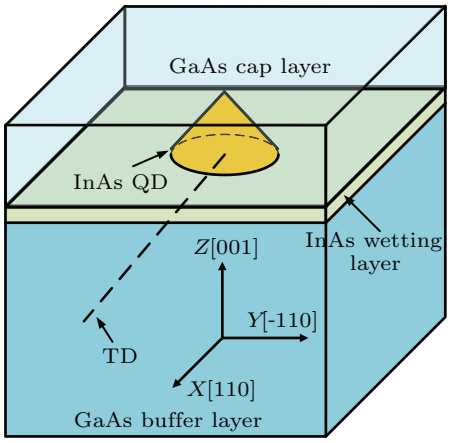


Fig. 1. Geometrical model of InAs/GaAs QD.

In this system, the lattice mismatch stresses $\boldsymbol{\sigma}_0^{ij} = (a_s - a_{QD})/a_{QD}\boldsymbol{C}\boldsymbol{\delta}_{ij}$ $(i,j = x,y,z)$ are exerted on QD, where a_s and a_{QD} ($a_s = 5.653$ Å, $a_{QD} = 6.058$ Å) are the lattice constants of the substrate and the QD, respectively. The elastic matrix of InAs $\boldsymbol{C}$[27–29] is expressed as

$$\boldsymbol{C} = \begin{bmatrix} 103.945 & 24.745 & 45.4 & 0 & 0 & 0 \\ 24.745 & 103.945 & 45.4 & 0 & 0 & 0 \\ 45.4 & 45.4 & 83.29 & 0 & 0 & 0 \\ 0 & 0 & 0 & 39.6 & 0 & 0 \\ 0 & 0 & 0 & 0 & 39.6 & 0 \\ 0 & 0 & 0 & 0 & 0 & 18.945 \end{bmatrix}.$$

The unit of each component in this matrix is in GPa. The non-singular, self-consistent formulas are adopted to simulate the TD segment[30] with Burgers vector expressed as $\left[\sqrt{(3/8)}a_s,\ \sqrt{(3/8)}a_s,\ a_s/2\right]$ and line vector [001], respectively.

Assume that there are two cases (1: TD enters into QD, 2: TD inclination occurs), as shown in Fig. 2. The elastic strain energy of the whole structure is calculated by varying the arrival position of TD in QD base width. Then the critical position and the bending area ratio of single QD can be obtained when the energy of the two systems is equal.

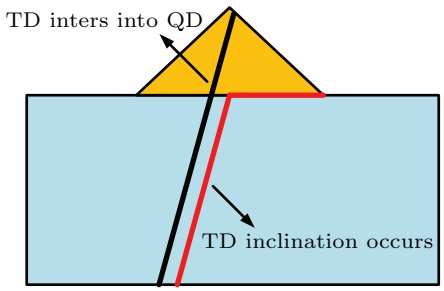


Fig. 2. Two cases when TD arrives at base of QD.

There is the stress caused by lattice mismatch and the stress induced by TD when TD enters into QD. The well-known equation is adopted to calculate the elastic strain energy of the system.[22,27,31] In addition to the above two kinds of stress sources, the stress induced by MD should be taken into consideration, and thus the equation needs adjusting appropriately[22,31] and the corresponding elastic strain energy in this system can be computed. To make the solution convergent, the appropriate boundary conditions are imposed, and a reasonable numerical value is obtained.

Through the calculation of the critical condition, we can obtain the bending area ratio A of single QD and the bending area ratio of single-layer QD M_1 is inferred to be

$$M_1 = AS\rho, \tag{1}$$

where S is the base area of single QD, and ρ is the density of QDs. Assuming that the TDs are uniformly distributed in the GaAs substrate and TD inclination occurs only when it reaches close to QD (neglecting the stress released by QDs formation[24] and the interaction between TDs), the dislocation blocking ratio of n-layer QDs dislocation filter M_n can be calculated from the following equations:

$$M_2 = AS\rho\,(1-M_1)+M_1, \tag{2}$$

$$M_3 = AS\rho\,(1-M_2)+M_2, \tag{3}$$

$$\cdots, \tag{4}$$

$$M_n = AS\rho\,(1-M_{n-1})+M_{n-1}. \tag{5}$$

Based on the above equations, the relationship between the number of the QDs layer and the blocking dislocation ratio can be speculated.

3. Results and discussion

In this section, the relationship between dislocation position and the elastic strain energy of InAs/GaAs QDs in the two isolated systems is explored. Then the effects of the cap layer thickness and the base width are investigated. Finally, the bending capability of the single-layer QDs and the multi-layer QDs are discussed.

As shown in Fig. 3, the corresponding elastic strain energy $E_{\rm thr}$ (the elastic strained energy of the system when TD enters into QD) and $E_{\rm mis}$ (the elastic strained energy of the system when TD inclination occurs) for a QD with 20-nm base width are calculated by changing the arrival position of TD from center to the boundary of the QD along the X-axis direction. When the TD enters into the QD without MD formation (the black curve as shown in Fig. 3), it can be seen that the energy is significantly affected by the position TD reaching and it decreases as TD approaches to the edge of the QD. While the energy tends to fluctuate up and down slightly when TD inclination occurs (the red curve as shown in Fig. 3). Two curves intersect at 9 nm, which is considered to be the critical position. The left side of the intersection represents QD bending TD into interfacial MD, and then the bending area ratio (about 81%) can be further obtained. It is found that the TD bending occurs more easily when it reaches the center region of the QD. We speculate that this is due to the force QD loading on TD in the central region is stronger than that in the edge region, and MD is energetically favorable in this region.

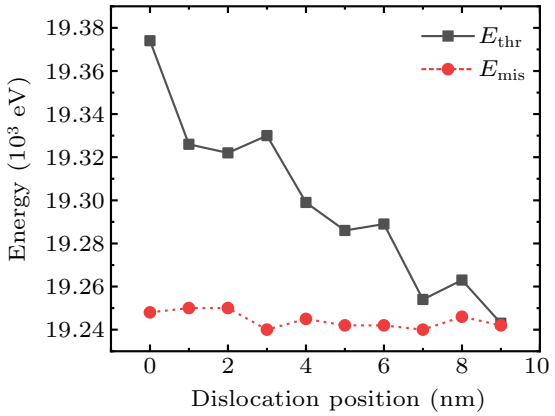


Fig. 3. The relationship of the stain energies $E_{\rm thr}$ and $E_{\rm mis}$ with the dislocation position.

In order to explore the influence of cap layer thickness for TD bending, we fix the critical position in a range from 9 nm to 9.8 nm, then the cap layer thickness is adjusted to make $E_{\rm thr}$ and $E_{\rm mis}$ equal. It is indicated in Fig. 4 that the thickness of cap layer needs increasing with the critical position moving rightward. With the bending area ratio of single QD raised from 81% to 96%, the required thickness must increase from an initial value of 5 nm to 9.2 nm. And the computations show that $E_{\rm thr}$ is much larger than $E_{\rm mis}$ in the whole range of QD base when the thickness of cap layer exceeds 10 nm. The result shows that heightening the thickness of cap layer can benefit the inclination of TD energetically, and this thickness selected in experiment to be almost more than 20 nm[18–20] is perfect enough.

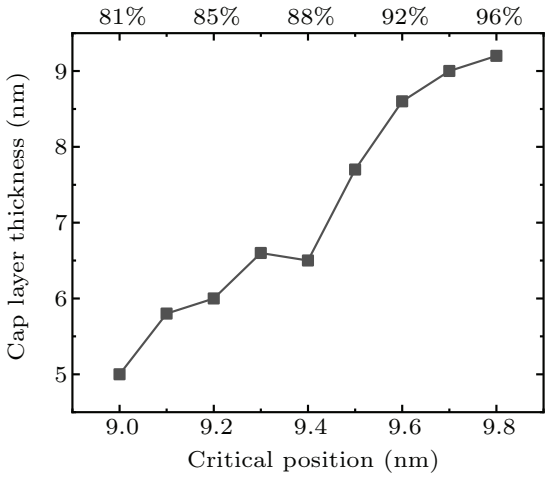


Fig. 4. Relationship between cap layer thickness and critical position.

Varying the base width from 8 nm to 24 nm and considering the 5-nm cap layer thickness, the E_{thr} and E_{mis} are calculated, and the results show that the relationship between the base width of QD and the bending area ratio of single QD is obtained. It can be seen from Fig. 5 that the bending area ratio shows an overall upward trend in this interval, but a slight decrease at 14 nm. This ratio increases rapidly from 8 nm to 12 nm, and it goes up steadily from 14 nm to 20 nm. Within the range of the base width, the maximum bending area ratio reaches 85.56%. The changing pattern is well consistent with the analytical results[20] (red points in the figure). However, there are some differences in quantitative value since we take TD position and cap layer into consideration.

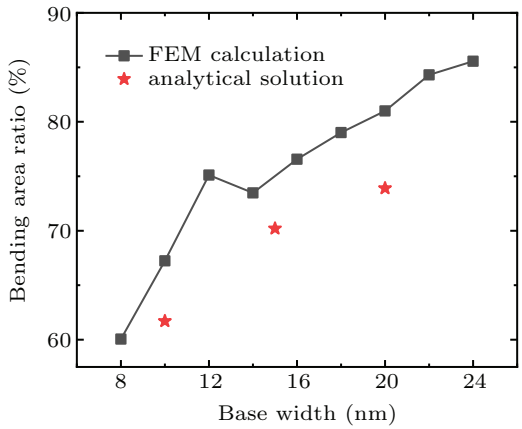


Fig. 5. The relationship between bending area ratio and base width of the single QD.

By using Eq. (1) and taking the density of 10^{11} cm^{-2} into account, the bending area ratio *versus* base width of single-layer QDs is calculated and shown in Fig. 6. The result shows that the bending area ratio keeps an upward tendency when the base width increases from 8 nm to 24 nm, and it rises up first slowly then rapidly in this range. The bending area ratio reaches its maximum value at 24 nm, *i.e.*, roughly 38.71%. This is similar to the calculation result reported previously[20] (red points in the figure).

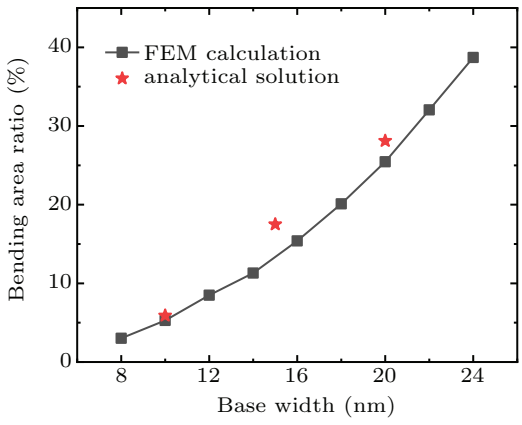


Fig. 6. Relationship between bending area ratio and base width of QD of single-layer QD.

Also following Eqs. (2)–(5), the dislocation blocking ratio is predicted with taking a base width of 24 nm. The results are shown in Fig. 7, indicating that the dislocation blocking ratio increases with the layer number of QDs rising from one to five. But unlike the bending area ratio of single layer, the increase is gradually slow down and tends to be saturated. When the number of the layers is five, the blocking dislocation ratio rises up to 91.35%. This regular pattern demonstrates that about 3–5 embedded QD layers can reduce the QDs density sufficiently, which can be proven by the previous experimental results.[19,20]

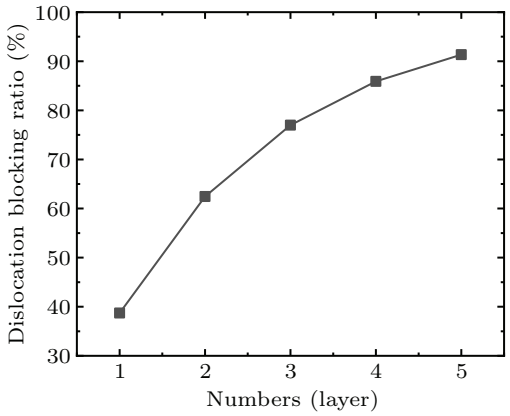


Fig. 7. The relationship between blocking dislocation ratio and layer number of QD.

4. Conclusions

In this work, the TD bending with InAs/GaAs QDs is studied. The results show that TD bending is more likely to occur in the central area of QDs, and its critical position is about 9 nm, corresponding to the height and width of the QD of 4 nm and 20 nm, respectively. The TD bending can be strengthened by increasing the cap layer thickness and the base width. In addition, the method to calculate the bending area ratio of single-layer QDs and the blocking dislocation ratio of multi-layers QDs are proposed. For QDs with a density of 10^{11} cm^{-2} and a base width of 24 nm, the bending area ratio of single-layer QDs reaches 38.71%, and the blocking dislocation ratio rises up to 91.35% when using the five-layer embedded QDs. This research can accurately evaluate the bending effect at the beginning of the experiment, and thus providing reasonable guidance for designing the QD dislocation filter. Although this study is about 60° TD with InAs/GaAs QD, its method is also applicable to other systems with reasonable modification.

References

[1] Liang D and Bowers J E 2010 *Nat. Photon.* **8** 511
[2] Rickman A 2014 *Nat. Photon.* **8** 579
[3] Miller D A B 2009 *Proc. IEEE.* **97** 1166
[4] Reed G T, Mashanovich G, Gardes F Y and Thomoson D J 2010 *Nat. Photon.* **4** 518
[5] Won R 2010 *Nat. Photon.* **4** 498
[6] Bahram J and Fathpour S 2006 *J. Lightw. Technol.* **24** 4600
[7] Yamaguchi M and Amano C 1985 *J. Appl. Phys.* **58** 3601
[8] Huang H, Ren X M, Lv J H, Wang Q, Song H L, Cai S W, Huang Y Q and Qu B 2008 *J. Appl. Phys.* **104** 113114

[9] Wang J, Hu H Y, He Y R, Deng C, Wang Q, Duan X F, Huang Y Q and Ren X M 2015 *Chin. Phys. Lett.* **32** 088101
[10] Wang Y F, Wang Q, Jia Z G, Li X Y, Deng C, Ren X M, Cai S W, and Huang Y Q 2013 *J. Vac. Sci. Technol. B* **31** 051211
[11] Lee S C, Dawson L R, Huang S H and Brueck S R J 2011 *Cryst. Growth Des.* **11** 3673
[12] Cheng S F, Gao L, Woo R L, Pangan A, Malouf G, Goorsky M S, Wang K L and Hicks R F 2008 *J. Cryst. Growth* **310** 562
[13] Kazi Z I, Egawa T, Jimbo T and Umeno M 1999 *IEEE Photon. Technol. Lett.* **11** 1563
[14] Lee S C and Brueck S R J 2009 *Appl. Phys. Lett.* **94** 153110
[15] Grundmann M, Stier O and Bimberg D 1995 *Phys. Rev. B* **52** 11969
[16] Grundmann M, ledentsov N N, Heitz R, Eckey L, Christen J, Bohrer J, Bimberg D, Ruvimov S S, Werner P, Richter U, Heydenreich J, Ustinov V M, Egorov A Yu, Zhukov A E, Kopev P S and Alferov Zh L 1995 *Phys. Status Solidi B* **188** 249
[17] Cusack M, Briddon and Jaros M 1996 *Phys. Rev. B* **54** R2300
[18] Yang J, Bhattacharya P and Mi Z 2007 *IEEE Trans. Electron Dev.* **54** 2849
[19] Wang J, Hu H Y, Deng C, He Y R, Wang Q, Duan X F, Huang Y Q and Ren X M 2015 *Chin. Phys. B* **24** 028101
[20] Hu H Y, Wang J, He Y R, Liu K, Liu Y Y, Wang Q, Duan X F, Huang Y Q and Ren X M 2016 *Appl. Phys. A* **122** 588
[21] Ye H, Lu P, Yu Z Y, Zhou S and Liu Y M 2011 *Solid State Sci.* **13** 1809
[22] Zhou S, Liu Y M, Wang D L and Yu Z Y 2013 *Superlattices Microstruct.* **63** 29
[23] Gatti R, Marzegalli A, Zinovyev V A, Montalenti F and Miglio L 2008 *Phys. Rev. B* **78** 184104
[24] Benabbas T, Androussi Y and Lefebvre A 1999 *J. Appl. Phys.* **86** 1945
[25] Liu G R and Jerry Quek S S 2002 *Semicond. Sci. Technol.* **17** 630
[26] Mi Z, Yang J, Bhattacharya P and Huffaker D L 2006 *Electron. Lett.* **42** 121
[27] Zhou S, Liu Y M, Lu P F, Han L H and Yu Z H 2014 *J. Nanomater.* **2014** 1
[28] Liu Y M, Yu Z Y, Ren X M and Xu Z H 2008 *Chin. Phys. B* **17** 3471
[29] Ye H, Lu P F, Yu Z Y, Yao W J, Chen Z H, Jia B Y and Liu Y M 2010 *Chin. Phys. B* **19** 047302
[30] Wei C and Athanasios A 2006 *J. Mech. Phys. Solids* **54** 561
[31] Ye H, Lu P F, Yu Z Y, Jia B Y, Feng H and Liu Y M 2010 *Physica E* **42** 2402